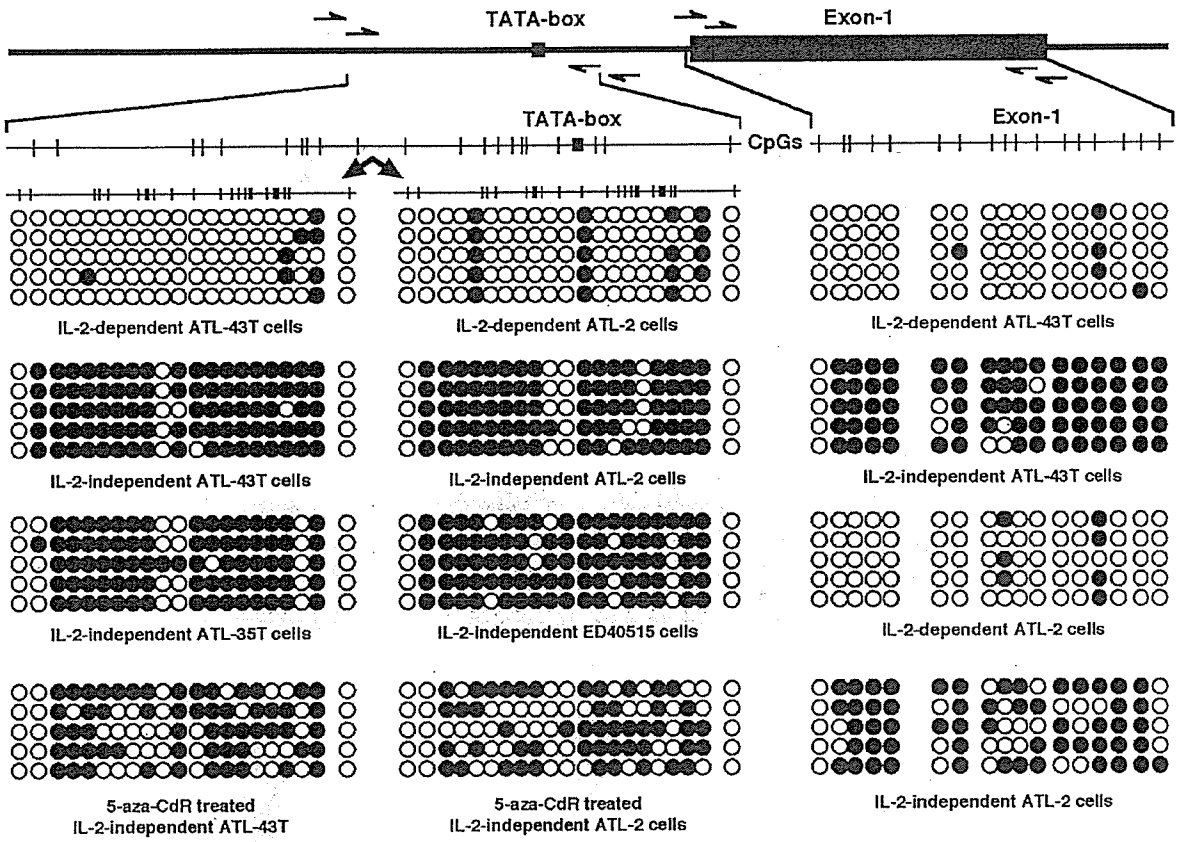

Figure 2 Methylation status of the thioredoxin-binding protein-2 (*TBP-2*) gene in HTLV-I-infected T-cell lines. Genomic DNA from HTLV-I-transformed IL-2-dependent and IL-2-independent cells before and after treatment with 5-aza-CdR were subjected to sodium bisulfite sequencing analyses as described in 'Materials and methods'. O, unmethylated CpG sites; •, methylated CpG sites.

for 3 days (Figure 3b, upper gel: lanes 3–5 and lanes 8–10), and further enhanced by additional treatment with SAHA for 1 day (Figure 3b, upper gel: lanes 6 and 11) in IL-2-independent ATL-43T and ATL-2 cells. The expression of TRX was not significantly altered by this treatment (Figure 3b, mid gel). These results suggested that both DNA-methylation and histone deacetylation synergistically silence the *TBP-2* gene in HTLV-I-infected IL-2-independent cells. In an earlier report (Butler *et al*., 2002), SAHA augmented TBP-2 expression through the CCAAT element of the *TBP-2* promoter. However, SAHA alone was unable to restore the TBP-2 expression in our cases. To clarify whether the effect of SAHA is a cancellation of histone deacetylation, we performed a chromatin immunoprecipitation (Chip) assay in IL-2-independent ATL-43T and ATL-2 cells. The PCR signal obtained using anti-acetylated-H3 or H4 antibody was very weak in IL-2-independent ATL-43T and ATL-2 cells, before treatment or on treatment with SAHA only (Figure 3c). After treatment with 5-aza-CdR, the PCR signal was markedly enhanced. Sequential treatment with 5-aza-CdR and SAHA further strengthened the PCR signal. These results strongly suggested that DNA methylation and histone deacetylation are synergistically involved in the *TBP-2* gene silencing in HTLV-I-infected IL-2-independent cell lines.

Association between downregulation of TBP-2 expression in response to IL-2 and cellular growth

Augmented TBP-2 expression results in growth suppression (Nishinaka *et al*., 2004a, b). We then analysed the relation between TBP-2 expression and growth in response to IL-2. We examined the level of TBP-2 expression and cell growth using [^{3}H]thymidine (Figure 4; ATL-43 T cells) and the MTT assay (Figure 5; ATL-2 cells). In IL-2-dependent ATL-43T (Figure 4a) and ATL-2 (Figure 5a) cells, TBP-2 expression was minimally maintained by the addition of IL-2, associated with cellular proliferation, whereas it was upregulated on deprivation of IL-2, associated with cell growth suppression. TBP-2 expression was recovered by sequential treatment with 5-aza-CdR and SAHA in IL-2-independent ATL-43T (Figure 4c) and ATL-2 (Figure 5c) cells. The expression of TBP-2 was also quantitated using real time RT–PCR (Figures 4d and 5d). These cells displayed a similar pattern of TBP-2 expression and growth in response to IL-2, mimicking that of IL-2-dependent cells. In contrast, IL-2-independent ATL-43T (Figure 4b) and ATL-2 (Figure 5b) cells

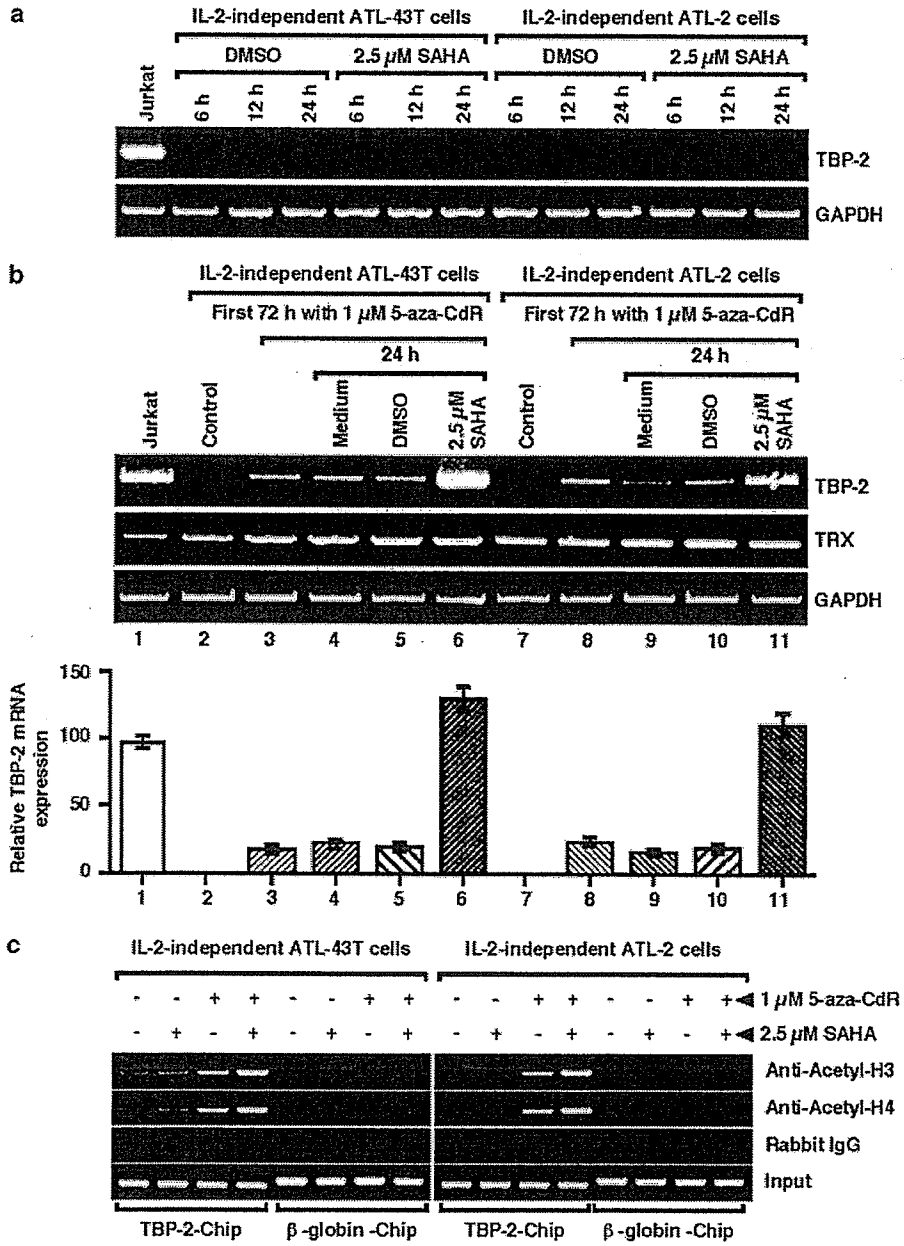

Figure 3 Restoration of thioredoxin-binding protein-2 (*TBP-2*) expression in interleukin-2 (IL-2)-independent HTLV-I-infected T cells by sequential treatment with 5-aza-2′-deoxycytidine (5-aza-CdR) and suberoylanilide hydroxamic acid (SAHA). (a) TBP-2 expression in SAHA-treated IL-2-independent ATL-43 T and ATL-2 cells. The cells were treated with 2.5 μM SAHA at the indicated time points and analysed by semiquantitative RT–PCR. (b) TBP-2 and TRX expression in the cells sequentially treated with 5-aza-CdR and SAHA. The cells were treated with 1 μM 5-aza-CdR for the first 72 h, then with complete medium, DMSO, or 2.5 μM SAHA for 24 h. The bar graph shows mean values of real-time RT–PCR from three replicates. Similar results were obtained in three separate experiments. Error bars represent s.d. 18S ribosomal mRNA expression was used as a cDNA loading control. (c) The histone acetylation status of the *TBP-2* promoter region (TBP-2-Chip) and *β-globin* (β-globin-Chip) determined by chromatin immunoprecipitation (Chip) assay. Assays were performed three times with the indicated antibodies, followed by PCR analysis.

proliferated well regardless of IL-2. In these cells, TBP-2 expression was completely abrogated and the cell growth did not change in response to IL-2. In Figure 4e (ATL-43T) and Figure 5e (ATL-2), statistical analysis of the day-3 data showed a significant ($P<0.05$) difference in growth between the presence and absence of IL-2 in IL-2-dependent cells and sequentially treated IL-2-independent cells, but not in untreated IL-2-independent cells. These results suggested that restored TBP-2 expression is associated with the response to IL-2 and suppression of uncontrolled IL-2-independent growth.

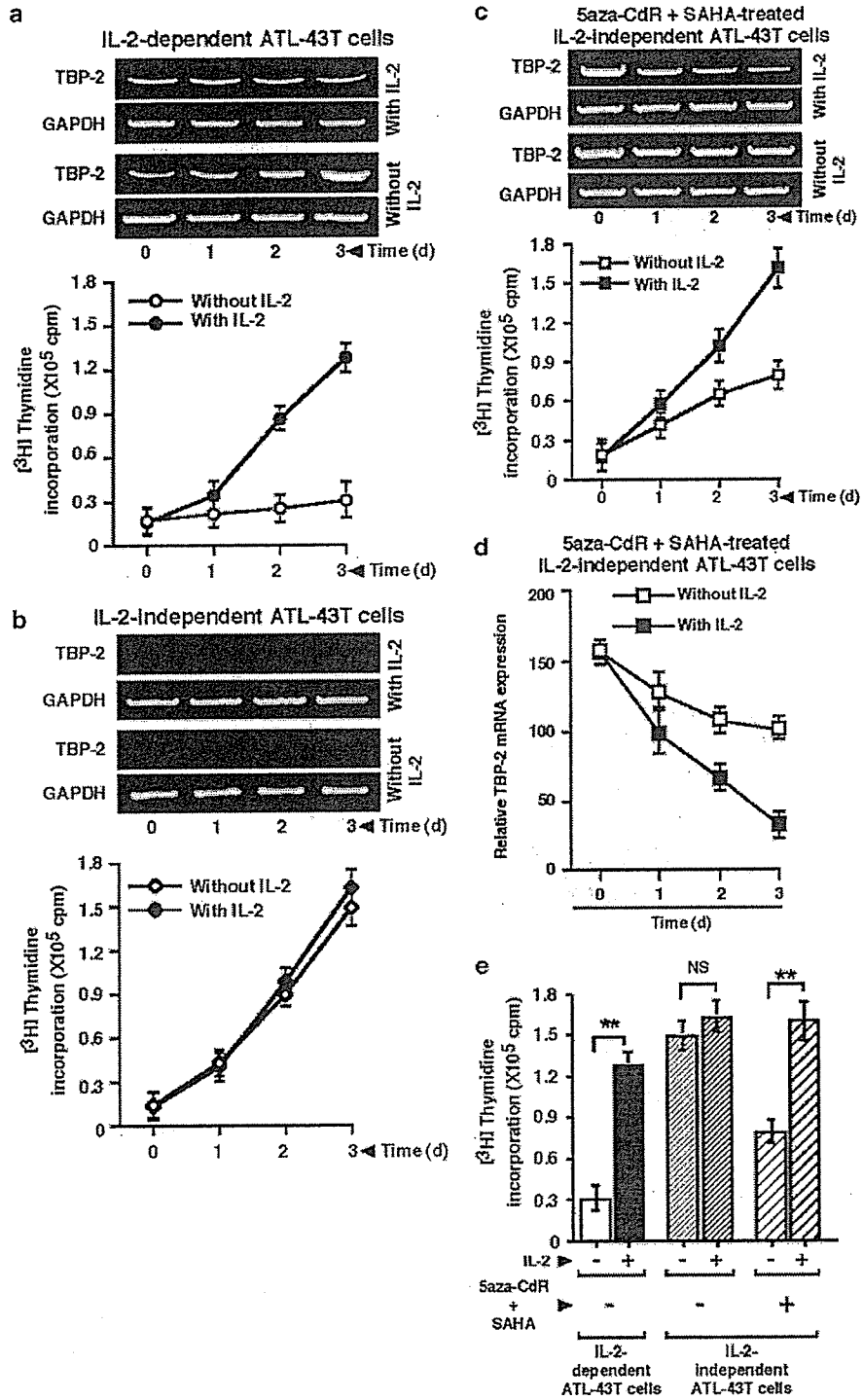

Figure 4 Thioredoxin-binding protein-2 (TBP-2) expression and cell growth in response to interleukin-2 (IL-2) in ATL-43T cells. The cells were cultured for 3 days in the absence or presence of IL-2 and cell growth was analysed using the thymidine incorporation assay. The expression of TBP-2 was analysed by semiquantitative RT–PCR. (a) IL-2-dependent ATL-43T cells, (b) IL-2-independent ATL-43T cells, and (c) IL-2-independent ATL-43T cells after sequential treatment with 5-aza-CdR and SAHA. (d) Quantitative real-time RT–PCR analysis of TBP-2 mRNA expression in the samples of Figure 4c. Data are representative of three separate experiments and the mean±s.d. from three replicates. (e) Statistical analysis of the day-3 data. Data are representative of three separate experiments and the mean±s.d. from three replicates. Nonsignificant and significant ($P<0.05$) differences are indicated by NS and (**), respectively, as determined with Student's *t* test.

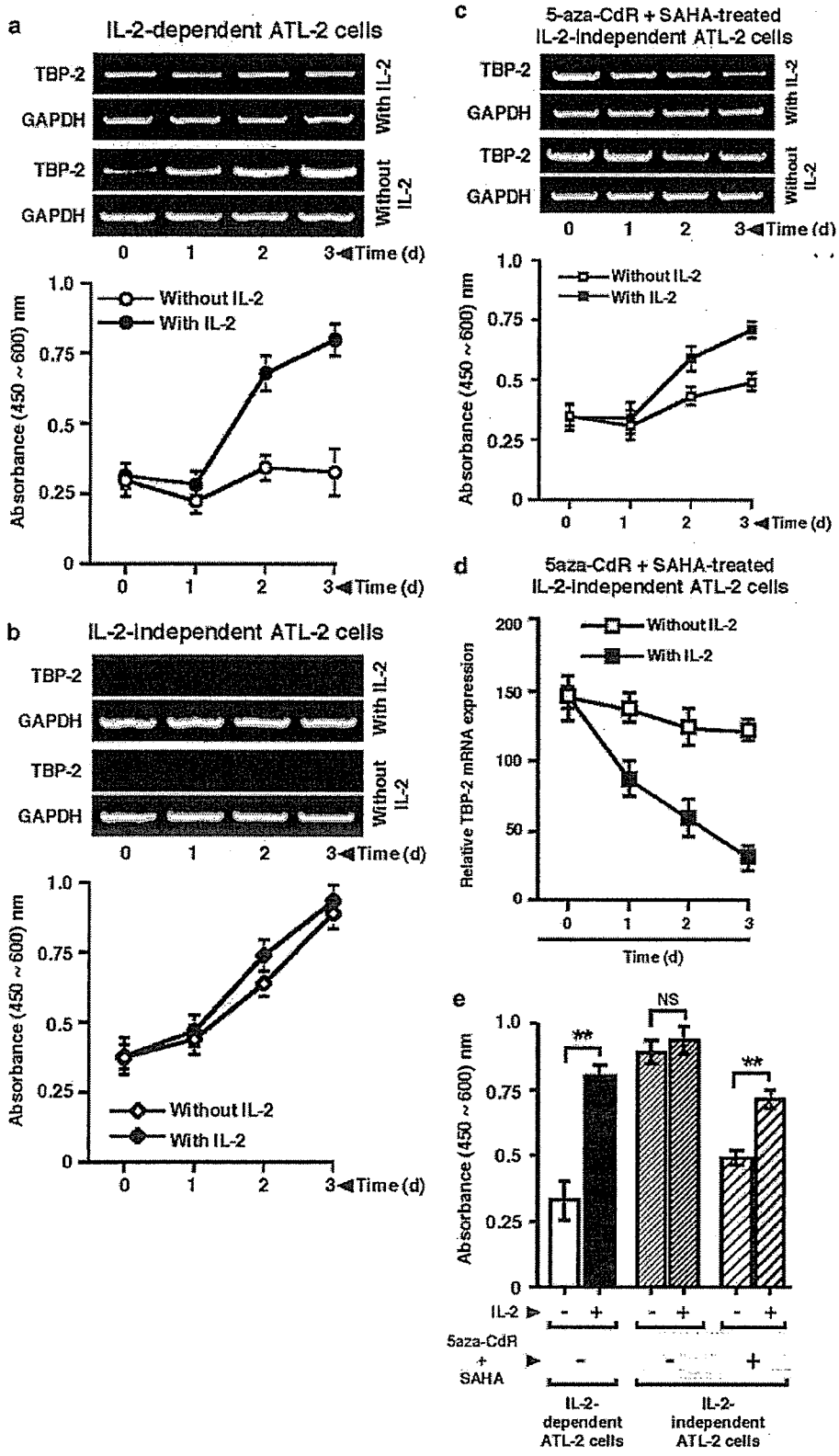
a
IL-2-dependent ATL-2 cells
TBP-2
GAPDH
With IL-2
Without IL-2
0 1 2 3 Time (d)
Absorbance (450 ~ 600) nm
Without IL-2
With IL-2
b
IL-2-Independent ATL-2 cells
c
5-aza-CdR + SAHA-treated
IL-2-Independent ATL-2 cells
d
5aza-CdR + SAHA-treated
IL-2-Independent ATL-2 cells
Relative TBP-2 mRNA expression
Time (d)
e
NS
**
IL-2
5aza-CdR + SAHA
IL-2-dependent ATL-2 cells
IL-2-independent ATL-2 cells

Ectopic expression of TBP-2 suppressed cell growth and partially restored IL-2 responsiveness

To further analyse the role of TBP-2 in the response to IL-2, we utilized HTLV-I-transformed MT-2 cells ectopically expressing TBP-2 (Nishinaka *et al.*, 2004a). TBP-2 protein expression in these transfectants was confirmed (Figure 6a). While the control clones C_1 and C_4 proliferated well regardless of IL-2, the TBP-2-overexpressing clones T_1 and T_2 proliferated less without IL-2 than with IL-2 ($P<0.05$; Figure 6b). Addition of IL-2 suppressed the expression of TBP-2 in TBP-2-overexpressing clones T_1 and T_2 (Figure 6b; Agarose gel snaps). These results suggested that the TBP-2 expression suppressed cell growth and partially restored responsiveness to IL-2. We further analysed the relationship between TBP-2 expression and IL-2-dependency in IL-2-dependent ATL-43T and ATL-2 cells by knocking down TBP-2 expression using RNA-interference (RNAi). The expression of TBP-2 was downregulated in these cells after the transfection with RNAi of TBP-2 but not with control RNAi (Figure 6c). The cells transfected with nonsilencing control RNAi proliferated in the presence of IL-2 but not in the absence of IL-2, while those cells transfected with TBP-2 RNAi showed partial proliferation in the absence of IL-2 (Figure 6d). These results suggest that loss of TBP-2 expression causes HTLV-I-infected IL-2-dependent cells to acquire a partial capability for growth without IL-2.

Discussion

We revealed that in IL-2-independent cells, the expression of TBP-2 is completely silenced due to DNA methylation and histone deacetylation (Figures 1–3). DNA methylation and histone deacetylation with the downregulation of gene expression for tumor suppressors such as CDKN2A, p53, E-cadherin and VHL tumor suppressor have been also reported (Ushijima and Okochi-Takada, 2005). TBP-2 is a regulator of the cell cycle and apoptosis (Butler *et al.*, 2002; Nishinaka *et al.*, 2004a). The *TBP-2* gene is downregulated during oncogenesis (Butler *et al.*, 2002; Han *et al.*, 2003), reported as a suppressor of melanoma metastasis (Goldberg *et al.*, 2003), and implicated in tumor progression in TBP-2 knockout mice (Oka *et al.*, in preparation). Therefore, the *TBP-2* gene seems to be an onco-suppressive gene. An HDAC inhibitor, SAHA, did not augment TBP-2 expression alone but induced the expression only after the reversal of DNA methylation (Figure 3a and b). Demethylation slightly induced histone acetylation (Figure 3c). These results indicate a link between DNA methylation and histone deacetylation, consistent with previous reports (Coombes *et al.*, 2003; Satoh *et al.*, 2003).

In HTLV-I-infected IL-2-dependent cells as well as murine IL-2-dependent CTLL-2 cells (data not shown), TBP-2 mRNA expression was upregulated on the deprivation of IL-2 and cells did not grow, whereas the expression was downregulated to within the normal range on the addition of IL-2 and cells started to grow, as shown by the current study and elsewhere (Nishinaka *et al.*, 2004a). TBP-2 gene expression is also induced by treatment with vitamin D_3 (Chen and DeLuca, 1994), HDAC inhibitors (Butler *et al.*, 2002), and serum deprivation (Han *et al.*, 2003). Therefore, expression of the *TBP-2* gene seems to be transcriptionally induced under conditions associated with cell growth arrest. TBP-2 mRNA expression paralleled the protein level (Nishinaka *et al.*, 2004a). The level of TBP-2 showed an inverse correlation with cell growth in response to IL-2 (Figure 4 and 5). TBP-2 may play a key role in the regulation of IL-2-dependent growth. TBP-2 gene regulation seems to be a sensor of deprivation of IL-2 signal. IL-2 deprivation upregulates TBP-2 expression transcriptionally, leading to cell growth arrest. Addition of IL-2 to the IL-2-deprived cells downregulates the expression of TBP-2 to the basal level, leading to proliferation. Therefore, loss of TBP-2 or loss of TBP-2 gene regulation causes loss of the growth control mechanism.

The ectopic expression of TBP-2 in MT-2 cells (Figure 6a) suppressed cell growth and restored the responsiveness to IL-2, although the response was partial (Figure 6b). Similarly, knockdown of TBP-2 by RNAi in IL-2-dependent cells (Figure 6c) caused a partial loss of IL-2-dependent growth control (Figure 6d). We consider the reason why TBP-2 overexpression only partially restored IL-2 dependence to be as follows. Since the transformation of HTLV-I seems to be a multistep process, TBP-2 alone may not be enough to restore the dependence on IL-2. In addition, the overexpressed *TBP-2* gene is less responsive to exogenous stimuli such as IL-2. The gene regulation of TBP-2 expression may be important for full IL-2-dependence. Overexpression of TBP-2 did not change the expression of the IL-2 receptor, or STAT binding activity (data not shown). Further study is needed to elucidate the mechanism of the regulation of TBP-2 expression in response to IL-2. The mechanism by which TBP-2 regulates growth suppression is under investigation. In our previous report, we observed a similar growth suppressive effect on overexpression of TBP-2 in other HTLV-I-transformed T cells (IL-2-independent

Figure 5 Thioredoxin-binding protein-2 (*TBP-2*) expression and cell growth in response to interleukin-2 (IL-2) in ATL-2 cells. The cells were cultured for 3 days in the absence or presence of IL-2 and cell growth was analysed by the MTT assay as described in 'Materials and methods'. The expression of TBP-2 was analysed by semiquantitative RT–PCR. (a) IL-2-dependent ATL-2 cells, (b) IL-2-independent ATL-2 cells, and (c) IL-2-independent ATL-2 cells after sequential treatment with 5-aza-CdR and SAHA. (d) Quantitative real-time RT–PCR analysis of TBP-2 mRNA expression in the samples of (c). Data are representative of three separate experiments and the mean ± s.d. from three replicates. (e) Statistical analysis of day-3 data. Data are representative of three separate experiments and the mean ± s.d. from three replicates. Nonsignificant and significant ($P<0.05$) differences are indicated by NS and (**), respectively as determined with Student's *t*-test.

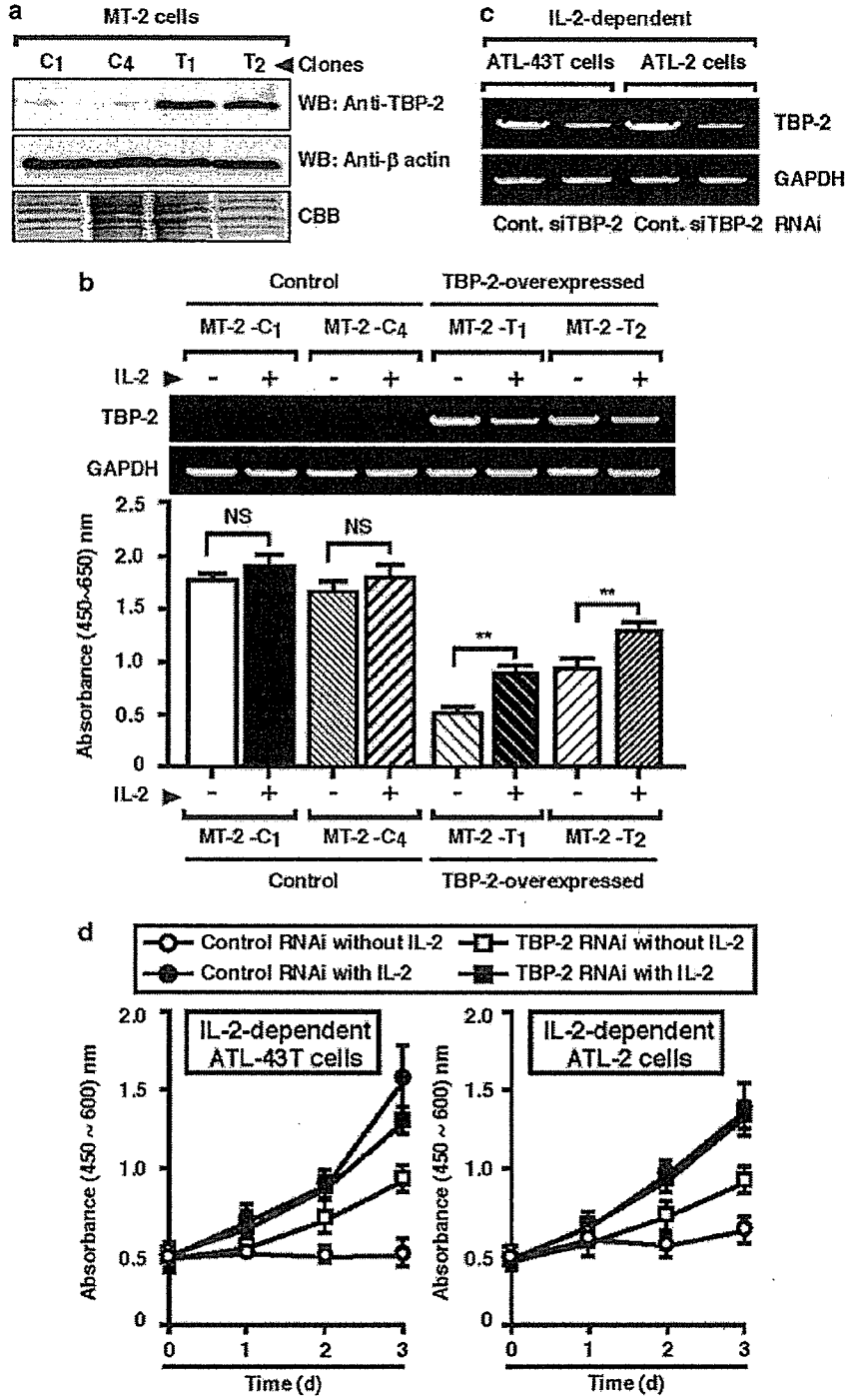

Figure 6 Relationship between TBP-2 expression and interleukin-2 (IL-2)-dependency in HTLV-I-infected T cells. (a) The MT-2 transfectants were stably transfected with *TBP-2* (T_1 and T_2) or control vector (C_1 and C_4) and the TBP-2 expression level was confirmed by Western blotting with monoclonal anti-TBP-2 antibody. Western blotting with monoclonal anti-β-actin antibody and staining with Coomassie Brilliant Blue R-250 (*CBB*) were used to monitor the amount of sample loaded. (b) Partial recovery of IL-2 dependency by overexpression of TBP-2. The TBP-2-overexpressing T_1 and T_2 or control C_1 and C_4 clones of MT-2 cells were cultured for 3 days in the absence or presence of IL-2 and cell proliferation was analysed by the MTT assay using WST-1 reagent. The upper panel shows the TBP-2 expression level analysed by semiquantitative RT–PCR. The cell proliferation data for day 3 in the absence or presence of IL-2 represent the mean$\pm$s.d. from three replicates. Similar results were obtained in three separate experiments. Nonsignificant and significant ($P<0.05$) differences are indicated by NS and (**), respectively, as determined with Student's *t*-test. (c) The expression of TBP-2 in cells transfected with RNAi of TBP-2. The level of TBP-2 was analysed by semiquantitative RT–PCR after 48 h of transfection. (d) IL-2-independent growth by knockdown of TBP-2 in HTLV-I-infected IL-2-dependent cells. After transfection with RNAi of TBP-2 or control, the cells were cultured for 3 days in the absence or presence of IL-2 and cell growth was analysed by MTT assay as described in 'Materials and methods'. The same results were obtained from three separate experiments.

ATL-43 T, ATL-2, and MT-2 cells). We also reported the disappearance of TBP-2 expression in Hut-102, ATL-2, MT-1 and MT-2 cells (Nishinaka *et al.*, 2004a), showing the generality of the finding in HTLV-I-infected cells. Loss of TBP-2 expression may augment the reducing activity of TRX (Nishiyama *et al.*, 1999), enhancing the growth of HTLV-I-infected T cells. In MT-2 cells ectopically expressing TBP-2, the expression of p16 was augmented (Nishinaka *et al.*, 2004a). Overexpression of TBP-2 also suppressed cell growth in MCF-7 cells, in which the p16 gene is deleted (Nishinaka *et al.*, 2004b), suggesting that there are other mechanisms to suppress cell growth. Analyses of gene expression in *TBP-2* knockout cells using Gene chips are underway. TBP-2 is localized to the nuclear compartment (Nishinaka *et al.*, 2004b). The interaction of TBP-2 with transcriptional repressors such as Fanconi anemia zinc-finger (FAZF), promyelocytic leukemia zinc-finger (PLZF) and HDAC1 has been suggested (Han *et al.*, 2003), and we have isolated several nuclear proteins that are important for the regulation of transcriptional events as partners of TBP-2 (Masutani *et al.*, in preparation). Therefore, it could be speculated that TBP-2, augmented by various stimuli, interacts with growth controlling molecules such as an HDAC complex to induce cell growth arrest.

In summary, we showed that the *TBP-2* gene is silenced due to DNA-methylation and histone deacetylation in IL-2-independent cell lines and that TBP-2 expression is closely associated with responsiveness to IL-2-dependent growth. The complete silencing of the *TBP-2* gene is seen in HTLV-I-infected IL-2-independent cells but not in other T-cell lines (Nishinaka *et al.*, 2004a), EBV-transformed cell lines, and other cell lines (unpublished observation). Therefore, the silencing may be specifically linked to the HTLV-I infection. Therefore, the role of the loss of TBP-2 expression seems more important in HTLV-I-infected leukemic cells. Although TBP-2 expression does not seem to be associated with Tax expression in the HTLV-I infected cell lines (data not shown), the role of viral proteins including Tax should be examined further. Clastogenetic changes (point mutations, deletions, substitutions, and translocations) are frequently found in HTLV-I-transformed cells. Disruption of base excision repair, nucleotide excision repair, DNA end stability, telomerase and cell cycle progression leads to an increase in the frequency of genomic mutation. ATL cells are convoluted and known to be aneuploid, suggesting an abnormality of the mitosis checkpoint in HTLV-I transformation (Jeang *et al.*, 2004). These aspects of HTLV-I transformation and ATL leukemogenesis are important. The role of loss of TBP-2 in these aspects of HTLV-I transformation should be also investigated further.

Materials and methods

Cell culture and transfections

Human lymphocytic leukemia T cells (Jurkat) and HTLV-I-infected T cells (ATL-2, MT-2, ED-40515, ATL-35T and ATL-43T) were cultured in RPMI-1640 medium containing 10% heat inactivated fetal calf serum (FCS) and antibiotics (penicillin 100 U/ml and streptomycin 100 μg/ml) at 37°C with 5% CO_2 in air. For the maintenance of IL-2-dependent HTLV-I-infected T cells, IL-2 (7.5 ng/ml; Peprotech EC) was added to the culture medium. HTLV-I-infected IL-2-dependent T cells, such as ATL-2, ED-40515, ATL-35T and ATL-43T), were established from ATL patients by culture in the presence of IL-2, whereas IL-2-independent cells were established by the long-term culture of IL-2-dependent cells (Maeda, 1992). Each set of IL-2-dependent and IL-2-independent cells has the same clonal origin as confirmed by the T-cell receptor-β gene rearrangement and HTLV-I proviral integration sites (Maeda, 1992). Stable MT-2 transfectants overexpressing TBP-2 were generated as described previously (Nishinaka *et al.*, 2004a) and maintained in medium containing 2 mg/ml of G418 (Nacalai Tesque).

Treatment of cells with 5-aza-CdR or SAHA

For the treatment with a demethylating reagent, IL-2-independent ATL-43T and ATL-2 cells were cultured in medium supplemented with 1 μM 5-aza-CdR (Sigma) for 3 or 5 days. For the treatment with HDAC inhibitors, cells were cultured in medium supplemented with 2.5 μM SAHA (Alexis Biochemicals). For the sequential treatment with the demethylating reagent and HDAC inhibitors, the cells were cultured in medium supplemented with 1 μM 5-aza-CdR for the first 3 days, then with 2.5 μM SAHA for the next 24 h. After the sequential treatment, the cells were cultured in the presence or absence of IL-2 (1U) for an additional 3 days. SAHA was dissolved in dimethyl sulfoxide (DMSO). After each treatment, cells were placed in fresh medium.

Measurement of TBP-2 mRNA expression by RT–PCR

For the TBP-2 mRNA expression analyses, total RNA was isolated from the cells using Trizol reagent (Invitrogen). cDNA was synthesized using a SuperScript First-Strand Synthesis System (Invitrogen) with oligo dT_{12-18}. The cDNA was amplified by PCR using a KlenTaq-LA DNA polymerase mix (Sigma). The primers used for the amplification were as follows: *TBP-2*, 5′-CCATGGTGATGTTCAAGAAGAT CAAG-3′ (forward) and 5′-CTCAGGGGCATACATAAA GA-3′ (reverse); *TRX*, 5′-ATGGTGAAGCAGATCGAG-3′ (forward) and 5′-TTAGACTAATTCATTAATGGT-3′ (reverse); *CDKN2A*, 5′-TTCGGCTGACTGGCTGGCCA-3′ (forward; exon 1) and 5′-AGCTCCTCAGCCAGGTCCAC-3′ (reverse; exon 2); and *glyceraldehydes-3-phosphate dehydrogenase (GAPDH)*, 5′-ATGGGGAAGGTGAAGGTCGGAG TC-3 (forward) and 5′-CCATGCCAGTGAGCTTCCCGTT C-3′ (reverse). PCR was performed under the following conditions: 32 cycles for *TBP-2* (denaturing at 94°C for 30 s, annealing at 53°C for 1 min, and extension at 72°C for 2 min), 20 cycles for *TRX* (denaturing at 94°C for 30 s, annealing at 50°C for 30 s, and extension at 72°C for 1 min), 30 cycles for *CDKN2A* (denaturing at 94°C for 30 s, annealing at 61°C for 45 s, and extension at 72°C for 1 min), and 22 cycles for *GAPDH* (denaturing at 94°C for 30 s, annealing at 61°C for 1 min, and extension at 72°C for 90 s). The PCR products were visualized by electrophoresis in 3% NuSieve GTG agarose (Cambrex Bio Science) gel.

Quantitative real-time RT–PCR

For measurement of the quantity of *TBP-2* mRNA, real-time RT–PCR was conducted with a TaqMan Universal Master Mix (Applied Biosystems) using reverse transcribed cDNA as a template, in triplicate. The amplification was performed

using an ABI Prism7000 under the following conditions: 50°C for 2 min and 95°C for 10 min, followed by 40 cycles (95°C for 15 s and 60°C for 1 min). The oligos and TaqMan probe for *TBP-2* were purchased from Applied Biosystems. 18S ribosomal RNA was used as an internal control.

Sodium bisulfite sequencing of genomic DNA
The genomic DNA was prepared from HTLV-I-infected IL-2-dependent or -independent cells using a Puregene DNA isolation kit (Gentra). Sodium bisulfite treatment was performed as reported previously (Nosaka *et al.*, 2000; Yasunaga *et al.*, 2004). For the sequencing of the *TBP-2* promoter region, 100 ng of genomic DNA was amplified by PCR using as primers, 5′-GGAGAAGACATCGGTCCT-3′ (forward) and 5′-CATGATGGAACTGAGTTGGT-3′ (reverse). For bisulfite-sequencing analyses, 100 ng of sodium bisulfite-treated genomic DNA was amplified by PCR using two pairs of methylation-specific primers. For the TATA-box region, a first round of amplification was performed with 5′-GGTTTTAGGGTTAGTGGGA-3′ (forward) and 5′-AAAAACCTTCTTTCCCCCAA-3′ (reverse), followed by a second round of nested PCR with 5′-TTTATTGGATTTGG GAGAA-3′ (forward) and 5′-ATCCAATCTCCACAAACA CTCC-3′ (reverse) primers. For the exon-1 region, a first round of amplification was performed with 5′-GGAAAGAA GGTTTTTTTTTTGA-3′ (forward) and 5′-CCACTTACCT ATTAACTAATCT-3′ (reverse), followed by a second round of nested PCR with 5′-TGATTTTGTTTAGTGTAATTAG-3′ (forward) and 5′-CCTATTAACTAATCTTCCAA-3′ (reverse). Amplification was carried out under the following conditions: 30 cycles (denaturing at 94°C for 30 s, annealing at 53°C for 1 min and extension at 72°C for 2 min), followed by a final extension at 72°C for 8 min. The PCR products were purified using a QIAEX II Gel extraction kit (Qiagen) and ligated into the vector pCR2.1 TOPO (Invitrogen). Inserts from five positive clones of each product were sequenced using M13 primers. Sequencing was performed using Big Dye Terminator reagent (Applied Biosystems) with an ABI PRISM310 Genetic Analyzer.

Chromatin immunoprecipitation (Chip) assay
For analyzing the histone acetylation status in TBP-2-restored cells, a Chip assay was performed as described previously (Spencer *et al.*, 2003). In brief, a chromatin solution was immunoprecipitated overnight at 4°C, using antiacetylated H3 and H4 antibodies (Upstate Biotechnology). Precipitated DNA was analysed by PCR amplification, using a KlenTaq LA DNA Polymerase Mix (Sigma). The following promoter-specific primers were used: *TBP-2* promoter region (207 bp); 5′-TCCAGAGCGCAACAACCAT-3′ (forward) and 5′-AAG CAGGAGGCGGAAACGT-3′ (reverse) or, *β-globin* promoter region (237 bp); 5′-GGCAAGGTGAACGTGGATG AAGTTGGTG-3′ (forward) and 5′-GGAGTGGACAGA TCCCCAAAGGACTCAAAG-3′ (reverse). PCR was carried out under the following conditions: 30 cycles for *TBP-2* (denaturing at 95°C for 30 s, annealing at 53°C for 1 min, and extension at 72°C for 2 min) or, 28 cycles for *β-globin* (denaturing at 95°C for 30 s, annealing at 66°C for 1 min, and extension at 72°C for 2 min). The PCR products were visualized by electrophoresis in 3% NuSieve GTG agarose gel.

Western blot
Cell lysates were prepared with lysis buffer (150 mM NaCl, 1% Triton X-100, 1 mM EDTA, 1 mM EGTA, 20 mM Tris-HCl (pH 7.5), 2.5 mM sodium pyrophosphate, 1 mM β-glycerophosphate, 1 mM sodium orthovanadate, 1 mM NaF and protease inhibitor cocktail (Roche)). Western blotting was performed as described previously (Nishinaka *et al.*, 2004a). The membrane was blocked with 10% (w/v) skim milk in Tris-buffered saline containing 0.05% Tween-20, then incubated with monoclonal anti-TBP-2 or anti-β-actin (Sigma, St MO) antibodies, followed by peroxidase-conjugated anti-mouse IgG (Amersham Biosciences, Tokyo, Japan). An ECL Western blot detection kit (Amersham, Tokyo, Japan) was used to visualize the epitopes.

Knockdown of TBP-2 expression by RNA interference (RNAi)
Double stranded oligonucleotides (rACAGACUUCGGA GUACCUGdTT) for selective silencing of *TBP-2* or control oligonucleotides (rUUCUCCGAACGUGUCACGUdTT) (Qiagen) were transfected into cells using a human T cell nucleofector kit (Amaxa biosystems, Tokyo, Japan). Eight hours after transfection, IL-2 was added to the culture.

Cell proliferation assay
To analyse the cellular growth, cell proliferation was assayed based on [^{3}H]-thymidine incorporation or with the MTT assay using WST-1 reagent (TaKaRa). Cells ($2–5 \times 10^3$/well) were seeded in 96-well flat-bottomed microtiter culture plates. Cells were cultured for 3 days in the presence or absence of IL-2 (7.5–15 ng/ml) and cell proliferation was assessed at different time points of the culture (day 0–3). For the [^{3}H]thymidine incorporation assay, cells were labeled with 1 μCi of [^{3}H]methyl-thymidine (Amersham) for the last 6 h and radioactivity was measured. For the MTT assay, cells were incubated with WST-1 reagent for the last 2 h and analysed with a Thermo-Max microplate reader.

Acknowledgements

We thank Dr Koichi Ikuta for discussions, and Ms Yoko Kanekiyo and Ms Satoko Maeji for secretarial assistance. This work was supported by a grant-in-aid for scientific research from the Ministry of Education, Culture, Sports, Science and Technology of Japan and by the Research and Development Program for New Bio-Industry Initiatives.

References

Butler LM, Zhou X, Xu WS, Scher HI, Rifkind RA, Marks PA *et al.* (2002). *Proc Natl Acad Sci USA* **99**: 11700–11705.
Cameron EE, Bachman KE, Myohanen S, Herman JG, Baylin SB. (1999). *Nat Genet* **21**: 103–107.
Chen KS, DeLuca HF. (1994). *Biochim Biophys Acta* **1219**: 26–32.
Coombes MM, Briggs KL, Bone JR, Clayman GL, El-Naggar AK, Dent SY. (2003). *Oncogene* **22**: 8902–8911.
Gardiner-Garden M, Frommer M. (1987). *J Mol Biol* **196**: 261–282.
Goldberg SF, Miele ME, Hatta N, Takata M, Paquette-Straub C, Freedman LP *et al.* (2003). *Cancer Res* **63**: 432–440.
Han SH, Jeon JH, Ju HR, Jung U, Kim KY, Yoo HS *et al.* (2003). *Oncogene* **22**: 4035–4046.
Holmgren A. (1985). *Annu Rev Biochem* **54**: 237–271.
Jeang KT, Giam C, Majone F, Aboud M. (2004). *J Biol Chem* **279**: 31991–31994.

Maeda M, Shimizu A, Ikuta K, Okamoto H, Kashihara M, Uchiyama T *et al.* (1985). *J Exp Med* **162**: 2169–2174.
Maeda M. (1992). *Hum Cell* **5**: 70–78.
Makino S, Masutani H, Maekawa N, Konishi I, Fujii S, Yamamoto R *et al.* (1992). *Immunology* **76**: 578–583.
Masutani H, Yodoi J. (2002). *Methods Enzymol* **347**: 279–286.
Matsuoka M. (2003). *Oncogene* **22**: 5131–5140.
Migone TS, Lin JX, Cereseto A, Mulloy JC, O'Shea JJ, Franchini G *et al.* (1995). *Science* **269**: 79–81.
Morgan DA, Ruscetti FW, Gallo R. (1976). *Science* **193**: 1007–1008.
Nishinaka Y, Nishiyama A, Masutani H, Oka S, Ahsan MK, Nakayama Y *et al.* (2004a). *Cancer Res* **64**: 1287–1292.
Nishinaka Y, Masutani H, Oka S, Matsuo Y, Yamaguchi Y, Nishio K *et al.* (2004b). *J Biol Chem* **279**: 37559–37565.
Nishiyama A, Matsui M, Iwata S, Hirota K, Masutani H, Nakamura H *et al.* (1999). *J Biol Chem* **274**: 21645–21650.
Nosaka K, Maeda M, Tamiya S, Sakai T, Mitsuya H, Matsuoka M. (2000). *Cancer Res* **60**: 1043–1048.
Okamoto T, Ohno Y, Tsugane S, Watanabe S, Shimoyama M, Tajima K *et al* (1989). *Jpn J Cancer Res* **80**: 191–195.
Satoh A, Toyota M, Itoh F, Sasaki Y, Suzuki H, Ogi K *et al.* (2003). *Cancer Res* **63**: 8606–8613.
Spencer VA, Sun JM, Li L, Davie JR. (2003). *Methods* **31**: 67–75.
Tagaya Y, Maeda Y, Mitsui A, Kondo N, Matsui H, Hamuro J *et al.* (1989). *EMBO J* **13**: 2244.
Uchiyama T, Yodoi J, Sagawa K, Takatsuki K, Uchino H. (1977). *Blood* **50**: 481–492.
Ushijima T, Okochi-Takada E. (2005). *Cancer Sci* **96**: 206–211.
Yasunaga J, Taniguchi Y, Nosaka K, Yoshida M, Satou Y, Sakai T *et al.* (2004). *Cancer Res* **64**: 6002–6009.
Yodoi J, Takatsuki K, Masuda T. (1974). *New Engl J Med* **290**: 572–573.
Yoshida M, Miyoshi I, Hinuma Y. (1982). *Proc Natl Acad Sci USA* **79**: 2031–2035.

Donor-Derived T-Cell Leukemia after Bone Marrow Transplantation

TO THE EDITOR: Asymptomatic carriers of human T-cell lymphotropic virus type I (HTLV-I) are considered acceptable as donors in allogeneic stem-cell transplantation for patients with adult T-cell leukemia–lymphoma (ATL).[1] However, the infusion of HTLV-I–infected cells from HTLV-I–seropositive donors could lead to the development of donor-derived ATL under immunosuppressive conditions after stem-cell transplantation. Here we describe a patient in whom ATL derived from donor cells developed four months after transplantation of stem cells from a sibling with HTLV-I.

A 44-year-old Japanese man with lymphoma-type ATL underwent transplantation of bone marrow from his HLA-identical brother in February 2004. The conditioning regimen included intravenous cyclophosphamide (120 mg per kilogram of body weight) and total-body irradiation (12 Gy). Cyclosporine and a short course of methotrexate were given as prophylaxis against graft-versus-host disease (GVHD). On day 26, low-dose prednisone was instituted because of GVHD-associated fever. With stable hematopoietic engraftment, complete donor chimerism was confirmed in a T-cell fraction on day 20 (Fig. 1). On day 133, the patient's white-cell count increased to 49.1×10^9 per liter with 89 percent ATL cells, although the original tumor had completely disappeared. Southern blot analysis revealed monoclonal integration of HTLV-I provirus in the ATL cells. Although we discontinued immunosuppressive therapy and administered chemotherapeutic agents, the patient died of the tumor in August 2004 (day 177).

A test for the status of donor–recipient chimerism in a T-cell–enriched fraction at the onset of ATL after transplantation showed a donor pattern (Fig. 1). In September 2004, hematologic and blood chemical values of the donor were almost normal, although the white-cell count included 1 percent atypical lymphocytes. Southern blot analysis showed no monoclonal integration of the HTLV-I provirus in the peripheral-blood mononuclear cells of the donor. These findings suggest that the donor was still an asymptomatic carrier without substantial clonal proliferation of HTLV-I–infected cells.

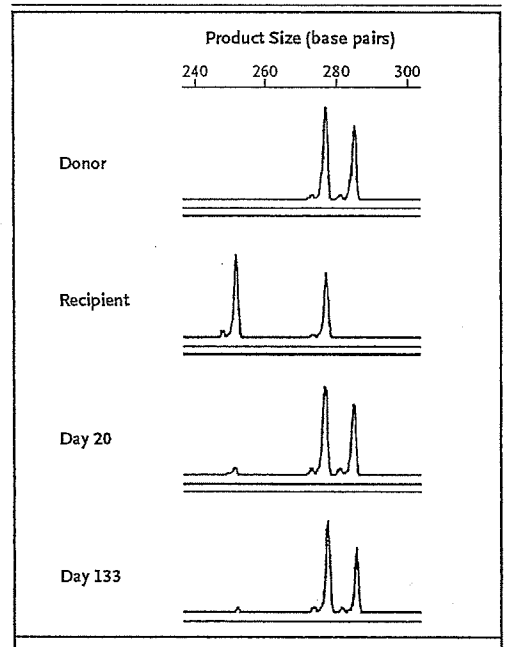

Figure 1. Analysis of T Cells at Engraftment (Day 20) and at the Onset of ATL (Day 133).

Genomic DNA from peripheral blood was amplified by polymerase-chain-reaction (PCR) assays with the use of fluorescent primers flanking an informative microsatellite region. Fluorescent peak controls for the donor and the recipient before stem-cell transplantation were obtained from whole peripheral-blood cells. At the onset of ATL after stem-cell transplantation, enriched CD3-positive cells, which were obtained with a purity of more than 95 percent, showed typical morphologic features of ATL cells on blood smears, and most of them expressed both CD4 and CD25, as assessed by flow cytometry. Fluorescent PCR products and GeneScan ROX 500 Size Standard were analyzed in a genetic analyzer with the use of Genescan software (Version 3.1.2) (ABI-310, Applied Biosystems).

Suppression of the host immune system increases the occurrence of virus-associated lymphoid cancers.[2] ATL develops in approximately 5 percent of HTLV-I carriers after an incubation period of several decades.[3] However, ATL has been reported to develop at a younger age in renal-transplant recipients with HTLV-I infection during immunosuppressive therapy[4] and sooner after the transmission of HTLV-I infection through blood transfusion in patients under immunosuppressive conditions.[5] Thus, the immunosuppressive

status in recipients of stem-cell transplants also potentially contributes to the development of ATL in donor-derived T cells that are infected with HTLV-I.

Hiroya Tamaki, M.D., Ph.D.
Osaka Minami Medical Center
Osaka 586-8521, Japan
tamaki@ommc-hp.jp

Masao Matsuoka, M.D., Ph.D.
Kyoto University Institute for Virus Research
Kyoto 606-8507, Japan

1. Utsunomiya A, Miyazaki Y, Takatsuka Y, et al. Improved outcome of adult T cell leukemia/lymphoma with allogeneic hematopoietic stem cell transplantation. Bone Marrow Transplant 2001; 27:15-20.
2. Cohen JI. Epstein–Barr virus infection. N Engl J Med 2000; 343:481-92.
3. Matsuoka M. Human T-cell leukemia virus type I and adult T-cell leukemia. Oncogene 2003;22:5131-40.
4. Hoshida Y, Li T, Dong Z, et al. Lymphoproliferative disorders in renal transplant patients in Japan. Int J Cancer 2001;91:869-75.
5. Chen YC, Wang CH, Su IJ, et al. Infection of human T-cell leukemia virus type I and development of human T-cell leukemia lymphoma in patients with hematologic neoplasms: a possible linkage to blood transfusion. Blood 1989;74:388-94.

A Case of Platydeoxia?

TO THE EDITOR: The Clinical Problem-Solving article by Hegland et al. (Dec. 1 issue)[1] concerned a case of platypnea–orthodeoxia, in which a positionally dependent intracardiac right-to-left shunt led to arterial desaturation when the patient was in the upright position but not the supine. We report a case in which the converse occurred.

An 81-year-old woman was brought to the emergency room by her neighbors, who found her lying on the floor of her apartment, markedly confused. On examination, the patient was cooperative but delirious. She was hemodynamically stable, her respiratory rate was 13 breaths per minute, and her initial oxygen saturation was 95 percent while breathing room air. Repeated oximetry several hours later revealed an oxygen saturation of 80 percent and blood gas measurement yielded a partial pressure of arterial oxygen (PaO_2) of 34 mm Hg that did not improve despite the delivery of high-flow oxygen by aerosol mask. The patient was intubated and transferred to the intensive care unit. A spiral computed tomographic scan was negative for pulmonary embolism but revealed a very large aneurysm in the ascending aorta (8.2 cm by 8.0 cm) that was compressing the right main pulmonary artery.

In the intensive care unit, the patient was placed in a sitting position and the PaO_2 increased to 486 mm Hg. Her PaO_2 remained elevated despite the reduction of the fraction of inspired oxygen (F_IO_2) to 35 percent, and she was extubated and transferred back to the ward. On the ward, her oxygen saturation dropped to 60 percent and rose only marginally while she was breathing supplemental oxygen. It was then noted that the oxygen saturation rapidly corrected to 100 percent when the patient was placed lying on her side or sitting upright. A transthoracic echocardiogram with bubble study was performed; it revealed a patent

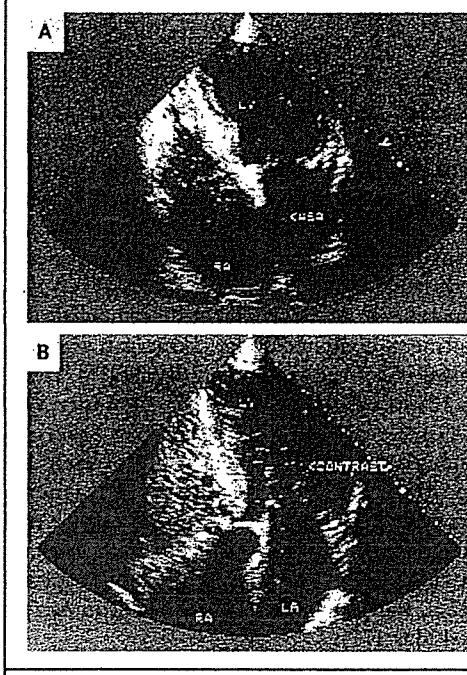

Figure 1. Transthoracic Echocardiography with Microbubble Contrast.

Panel A shows the echocardiogram that was obtained with the patient in the left lateral decubitus position and shows abundant microbubbles in the right atrium (RA) and only a few in the left ventricle (LV). ASA denotes atrial septal aneurysm. The echocardiogram in Panel B was obtained while the patient was in the supine position and shows the increased presence of microbubbles in the left atrium (LA) and left ventricle (LV).

Retrovirology

BioMed Central

Research

Open Access

Silencing of human T-cell leukemia virus type I gene transcription by epigenetic mechanisms

Yuko Taniguchi[1], Kisato Nosaka[1,2], Jun-ichirou Yasunaga[1], Michiyuki Maeda[3], Nancy Mueller[4], Akihiko Okayama[5] and Masao Matsuoka*[1]

Address: [1]Laboratory of Virus Immunology, Institute for Virus Research, Kyoto University, Kyoto 606-8507, Japan, [2]Department of Hematology, Kumamoto University School of Medicine, Kumamoto 860-8556, Japan, [3]Laboratory of Infection and Prevention, Institute for Virus Research, Kyoto University, Kyoto 606-8507, Japan, [4]Department of Epidemiology, Harvard School of Public Health, Boston, Massachusetts 02115, USA and [5]Department of Laboratory Medicine, Faculty of Medicine, University of Miyazaki, Miyazaki 889-1692, Japan

Email: Yuko Taniguchi - yutanigu@virus.kyoto-u.ac.jp; Kisato Nosaka - knosaka@fc.kuh.kumamoto-u.ac.jp; Jun-ichirou Yasunaga - jyasunag@virus.kyoto-u.ac.jp; Michiyuki Maeda - mimaeda@virus.kyoto-u.ac.jp; Nancy Mueller - nmueller@epinet.harvard.edu; Akihiko Okayama - okayama@med.miyazaki-u.ac.jp; Masao Matsuoka* - mmatsuok@virus.kyoto-u.ac.jp

* Corresponding author

Published: 22 October 2005

Retrovirology 2005, 2:64 doi:10.1186/1742-4690-2-64

Received: 31 August 2005
Accepted: 22 October 2005

This article is available from: http://www.retrovirology.com/content/2/1/64

Abstract

Background: Human T-cell leukemia virus type I (HTLV-I) causes adult T-cell leukemia (ATL) after a long latent period. Among accessory genes encoded by HTLV-I, the *tax* gene is thought to play a central role in oncogenesis. However, Tax expression is disrupted by several mechanims including genetic changes of the *tax* gene, deletion/hypermethylation of 5'-LTR. To clarify the role of epigenetic changes, we analyzed DNA methylation and histone modification in the whole HTLV-I provirus genome.

Results: The *gag*, *pol* and *env* genes of HTLV-I provirus were more methylated than pX region, whereas methylation of 5'-LTR was variable and 3'-LTR was not methylated at all. In ATL cell lines, complete DNA methylation of 5'-LTR was associated with transcriptional silencing of viral genes. HTLV-I provirus was more methylated in primary ATL cells than in carrier state, indicating the association with disease progression. In seroconvertors, DNA methylation was already observed in internal sequences of provirus just after seroconversion. Taken together, it is speculated that DNA methylation first occurs in the *gag*, *pol* and *env* regions and then extends in the 5' and 3' directions *in vivo*, and when 5'-LTR becomes methylated, viral transcription is silenced. Analysis of histone modification in the HTLV-I provirus showed that the methylated provirus was associated with hypoacetylation. However, the *tax* gene transcript could not be detected in fresh ATL cells regardless of hyperacetylated histone H3 in 5'-LTR. The transcription rapidly recovered after *in vitro* culture in such ATL cells.

Conclusion: These results showed that epigenetic changes of provirus facilitated ATL cells to evade host immune system by suppressing viral gene transcription. In addition, this study shows the presence of another reversible mechanism that suppresses the *tax* gene transcription without DNA methylation and hypoacetylated histone.

Background

Human T-cell leukemia virus type I (HTLV-I) is associated with a neoplastic disease, adult T-cell leukemia (ATL), and inflammatory diseases, such as HTLV-I-associated myelopathy (HAM)/tropical spastic paraparesis (TSP) and HTLV-I-associated uveitis [1,2]. Among HTLV-I carriers, a part of infected individuals develop ATL after a long latent period. During the leukemogenesis by HTLV-I, Tax protein is considered to play a critical role through its pleiotropic actions, which include transactivation of NF-κB, CREB and SRF pathways, transrepression of *lck*, *p18* and DNA polymerase β gene transcriptions, and functional inactivation of p53 and MAD1 [3-6]. Through these actions, Tax induces the proliferation of HTLV-I infected cells and inhibits their apoptosis, resulting in an increase in the number of infected cells. However, since Tax protein is the major target of cytotoxic T-lymphocytes (CTLs) *in vivo*, the expression also has a negative effect on the survival of ATL cells [7-9]. In some ATL cells, *tax* gene expression is inactivated by genetic and epigenetic changes, which include deletion, insertion or mutation of the *tax* gene, and DNA methylation or deletion of 5'-LTR [10-13]. Such inactivation of Tax expression is considered to allow ATL cells to escape from the host immune system.

DNA methylation of retroviruses is regarded as a host defense mechanism for inactivating retrovirus expression [14]. However, it is also recognized as a mechanism for virus-infected cells to escape from the host immune system and establish the latent state. In contrast, human immunodeficiency virus (HIV) is resistant to silencing *in vivo*. It is because HIV is frequently integrated into active transcriptional unit *in vivo* [15]. These findings coincide with the fact that HIV vigorously replicates *in vivo*. On the other hand, DNA methylation accumulated in HTLV-I 5'-LTR has been shown to silence viral gene transcription in leukemic cells [12,13]. In addition, the frequency of integration of HTLV-I provirus into transcriptional units was equivalent to that calculated based on random integration [16], which also increased the silencing. It remains unclear where and when DNA methylation occurs within the HTLV-I provirus genome.

In this study, we analyzed DNA methylation and histone modification in the whole HTLV-I provirus, and observed the progressive accumulation of DNA methylation. In addition, another reversible mechanism silenced viral gene transcription regardless of hyperacetylated promoter region.

Results

Analyses of DNA methylation of HTLV-I provirus

To reveal DNA methylation status within the HTLV-I provirus, we analyzed the DNA methylation by sodium bisulfite sequencing and combined bisulfite restriction analysis (COBRA). Initially, DNA methylation in 5'-LTR, gag, pol, env, pX and 3'-LTR was identified by sodium bisulfite sequencing. In an ATL case (Fig. 1A), the internal regions of the HTLV-I provirus, including gag, pol and env, were heavily methylated. On the other hand, 5'-LTR and pX were partially methylated, and 3'-LTR was not methylated at all. In an ATL cell line, ATL-48T (Fig. 1A), the internal sequences of the HTLV-I provirus were partially methylated, whereas both LTRs were not methylated. Since the analyses by sodium bisulfite sequencing were time-consuming, we established the COBRA method to detect and analyze DNA methylation in a large number of samples, and then compared the results obtained with the two methods. After amplification of sodium bisulfite treated DNAs with each primer sets, the products were digested with TaqI or AccII, which contain one (TaqI) or two (AccII) CpG site(s) within the recognition sequences. When CpG site is methylated, the products retain CpG site, resulting in digestion by these enzymes. On the other hand, CpG is converted to UG when it is unmethylated. Therefore, PCR products are resistant to restriction enzymes (Fig. 1B). With the COBRA method, the extent of DNA methylation was quantified in eight CpG sites throughout the HTLV-I provirus: 5'-LTR (620 according to the numbering by Seiki et al. [17]), gag (1753), pol (2988, 4187 and 5151), env (6113), pX (7258) and 3'-LTR (8342) (Fig. 1C). The extent of DNA methylation detected by the COBRA method was well correlated with that obtained by sodium bisulfite sequencing in both cases studied, as shown in Fig. 1A and 1C.

DNA methylation throughout the HTLV-I provirus in HTLV-I-transformed and ATL cell lines

Using the COBRA method, we analyzed the DNA methylation throughout the whole HTLV-I provirus of the cell lines (Fig. 2B and 2C). In addition, we also analyzed the tax gene transcription by RT-PCR (Fig. 2A) and the number of integrated HTLV-I proviruses in each cell lines by Southern blot method. Among the tax gene-expressing cell lines (ATL-35T, MT-2, Sez627, MT-4, ATL-55T, MT-1 ATL-48T and ATL-2) (Fig. 2A), internal sequences from gag to pX were variably methylated. However, 5'-LTR was not methylated or partially methylated, while 3'-LTR was not methylated in all cell lines (Fig. 2B). In ATL-43T and TL-Oml, which did not show tax gene transcription (Fig. 2A), 5'-LTR and the internal sequences were heavily methylated (Fig. 2C), indicating the close correlation between the extents of DNA methylation of the provirus, particularly 5'-LTR, and tax gene transcription. As previously reported, the treatment by 5-aza-deoxy-cytidine can recover the tax gene expression of these cell lines, indicating that the latent state by DNA methylation of 5'-LTR is reversible [13].

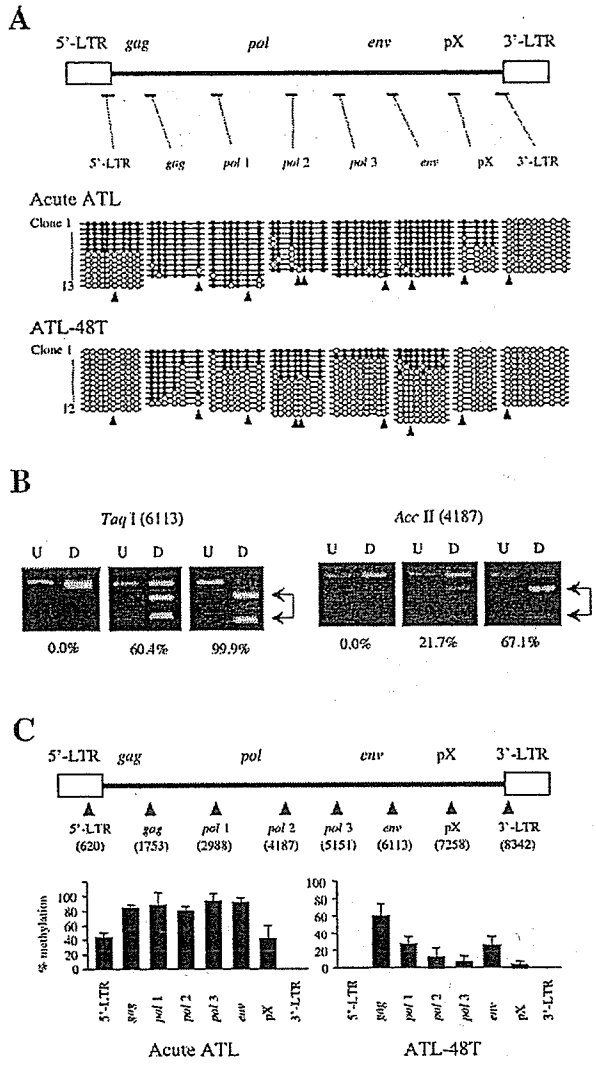

Figure 1

DNA methylation of the HTLV-I provirus assessed by sodium bisulfite sequencing and COBRA. A. DNA methylation in the HTLV-I provirus was analyzed by sodium bisulfite sequencing in a case of acute ATL and a *tax* gene-expressing cell line, ATL-48T. Eight DNA regions, which were represented as bars in A, were amplified with sodium bisulfite treated DNA. The PCR products were subcloned into plasmid DNA, and then the sequences of each clone were determined for at least ten clones of each region. Arrowheads indicate the CpG sites that were target sites for COBRA. Closed circle indicates methylated CpG, and open circle means unmethylated CpG. The number of integrated provirus has been shown in parenthesis. B. Representative data of COBRA has been shown. PCR products, which were amplified with sodium bisulfite treated DNAs, were digested with *Taq*I or AccII. The extent of methylation in each CpG site was measured as described in Methods, and presented as percentages of methylated CpG. The number in parenthesis represents the position of cytidine residue in analyzed CpG site by COBRA according to Seiki et al. [41]. C. DNA methylation studied by COBRA at eight points in the provirus as shown by arrowheads. Each bar represented the extent of DNA methylation at the points shown by arrowhead. The analyses by COBRA were performed three times independently, and the extents of DNA methylation are shown by the mean ± SD. The number in parenthesis shows the position of cytidine residue of CpG site analyzed by COBRA.

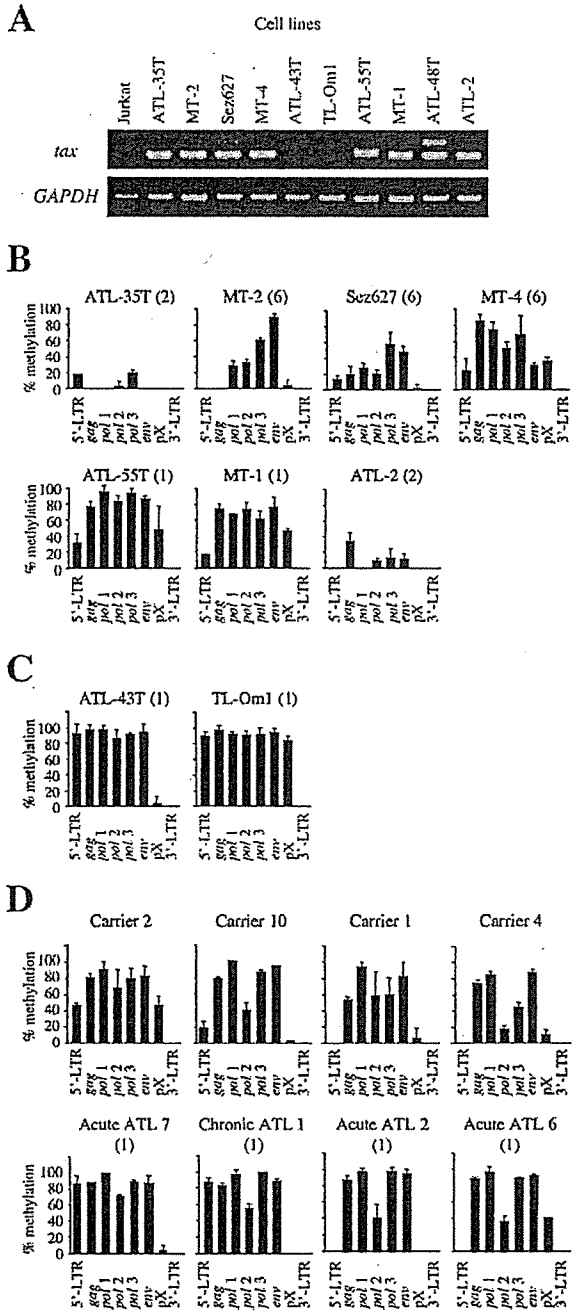

Figure 2

DNA methylation in ATL cell lines, HTLV-I carriers and ATL cases. The *tax* gene transcription in ATL cell lines was studied by RT-PCR (A), and the expression of *GAPDH* gene has been used as a control. DNA methylation throughout the HTLV-I provirus was studied by COBRA in *tax* gene-expressing (B) and non-expressing cell lines (C). Furthermore, DNA methylation was also analyzed in 20 carriers and 20 ATL cases by COBRA, and representative patterns of DNA methylation are shown in D. The number of HTLV-I provirus has been analyzed by Southern blot method, and shown in the parenthesis (B, C and D). Each bar indicates the extent of DNA methylation that was calculated by COBRA.

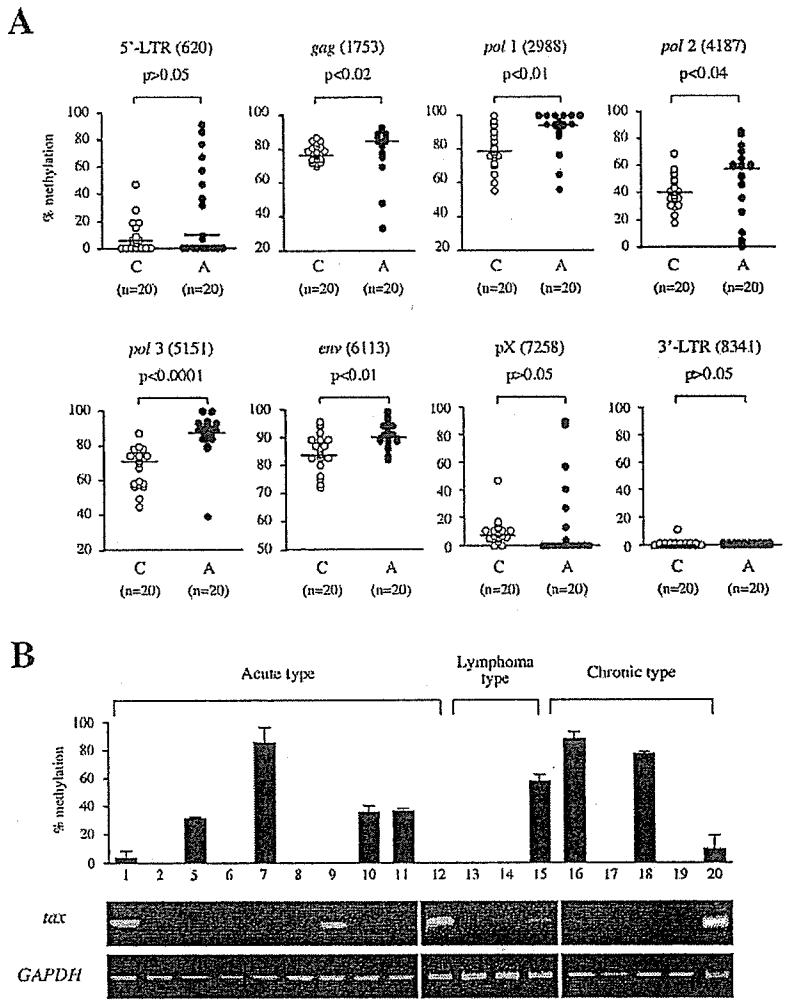

Figure 3

Comparison of the DNA methylation in carriers and ATL cases. A. DNA methylation at eight different regions in the HTLV-I provirus was compared between carriers (C) and ATL cases (A). DNA methylation was quantified by COBRA in 20 carriers and 20 ATL cases. Each sample was analyzed three times by COBRA at each site, and circles indicate mean values of DNA methylation. The differences of DNA methylation are statistically significant in the *gag*, *pol* and *env* regions by the Mann-Whitney's U-test. Horizontal bars represent median of DNA methylation in each group. B. The relation between *tax* gene transcription and DNA methylation of 5'-LTR in the fresh ATL cells has been shown. DNA methylation of 5'-LTR was quantified by COBRA assay and the *tax* gene transcripts were detected by RT-PCR.

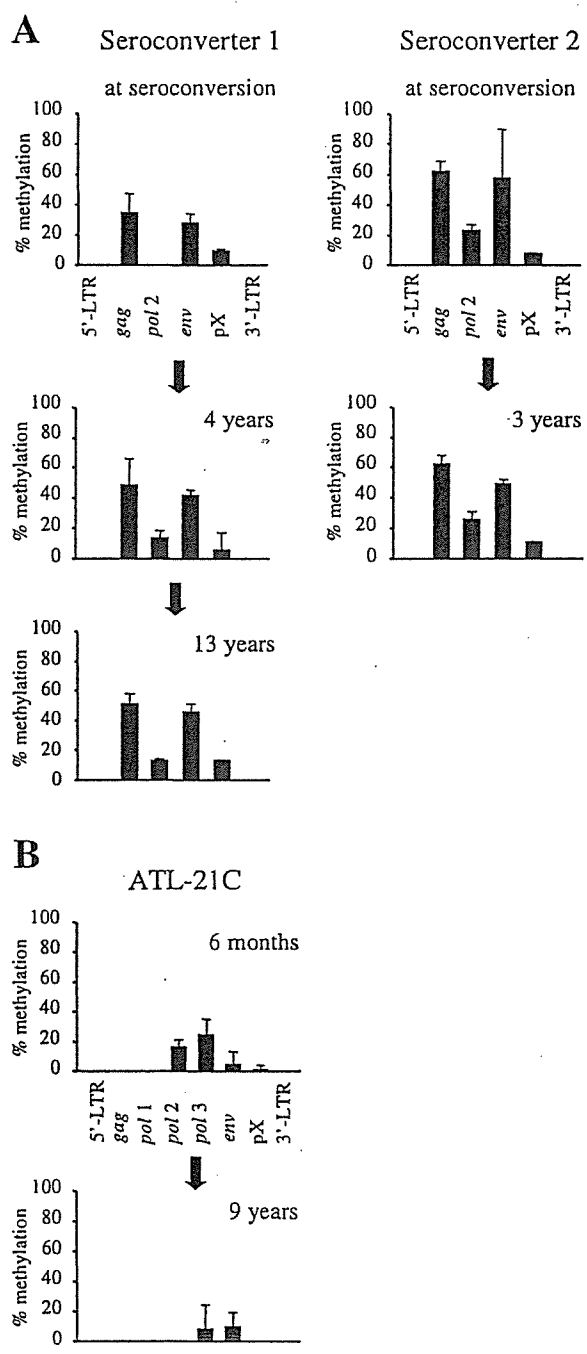

Figure 4
Sequential analyses of the DNA methylation in seroconverters and a cell line. DNA methylation was analyzed by COBRA in sequential samples from seroconverters (A) and in a cell line, ATL-21C, (B) cultured *in vitro* for more than 9 years. DNA methylation was analysed by COBRA three times, and each bar indicates mean ± SD.

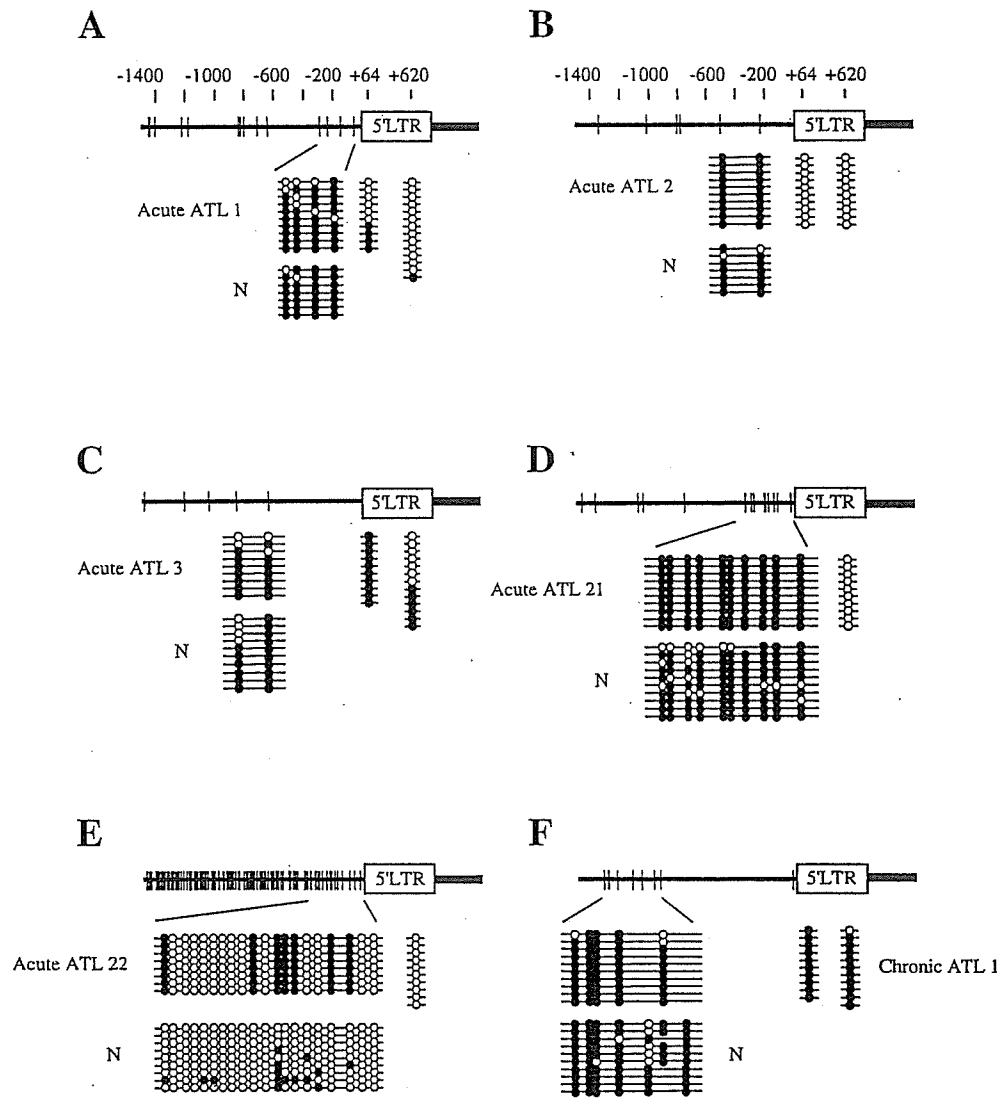

Figure 5

DNA methylation of provirus is not associated with methylated CpG sites in the genome. Integration sites of HTLV-I provirus in leukemic cells have been determined by inverse PCR, and then DNA methylation in genome has been analyzed by sodium bisulfite sequencing. DNA methylation of 5'-LTR was also analyzed by sodium bisulfite sequencing method. Vertical bars represent CpG sites. Open circle indicates unmethylated CpG site, and closed one means methylated CpG site. N: normal PBMCs from non-carrier donor.

Among cell lines, HTLV-I provirus tends to be not so methylated in cell lines with higher copy number of provirus (Fig. 2). The finding that cell lines with higher integrated provirus number contain hypomethylated provirus is speculated to reflect the higher transcription of viral genes.

DNA methylation of the HTLV-I provirus in ATL and HTLV-I carrier states

Next, we analyzed the DNA methylation of the whole HTLV-I provirus in ATL patients and HTLV-I carriers. Although 5'-LTR is frequently deleted in ATL cells [10], we omitted such ATL cases lacking 5'-LTR in this study. In Fig. 2D, we showed the representative pattern of DNA methylation of whole HTLV-I provirus in carriers and ATL patients. In ATL samples, the gag, pol and env regions were heavily methylated, whereas 5'-LTR was not methylated or partially methylated (Fig. 2D and 3A). On the other hand, 5'-LTR was scarcely methylated and the gag, pol and env regions seemed to be less methylated in HTLV-I carriers (Fig. 2D and 3A). We compared DNA methylation of these different eight regions between 20 carriers and 20 ATL cases (Fig. 3A). These differences in DNA methylation were statistically significant in the gag, pol and env regions between the ATL cases and HTLV-I carriers by the Mann-Whitney's U-test. These data suggested that DNA methylation initially occurred in the gag, pol, and env regions, and that DNA methylation of the provirus accumulated during disease progression from the carrier state to the leukemic stage. The frequency of DNA methylation of 5'-LTR did not differ between carriers and ATL patients. However, the extent of DNA methylation among methylation-positive cases was higher in ATL cases than in carriers ($p = 0.001$). Among ATL cases, the relationship between DNA methylation of 5'-LTR and tax gene transcription was analyzed (Fig. 3B), and the transcript was detected in six cases. In four cases with relative higher amount of tax gene transcripts (Case 1, 9, 12, 20), 5'-LTR was not methylated or slightly methylated. This finding suggests that higher expression of tax gene is associated with unmethyalted or slightly methylated 5'LTR, however, other mechanism(s) silences the tax gene transcription in ATL cells. There is no statistical correlation between the tax gene transcription and DNA methylation of 5'-LTR

DNA methylation of HTLV-I provirus after seroconversion

The analyses of DNA methylation suggest that it first occurs around the gag, pol and env regions, and then progresses in both the 5' and 3' regions. To study the changes in DNA methylation after infection, we analyzed sequential DNA samples from seroconverters. As shown in Fig. 4A, DNA methylation already existed in the gag, pol and env regions at the seroconversion. In seroconverter 1, DNA methylation was slightly increased at 4 and 13 years after the seroconversion. Increase of DNA methylation at pol region (4187) is statistically significant 13 years later in seroconverter 1 ($p = 0.02$, by a Student's t-test). On the other hand, there was little change in the DNA methylation in seroconverter 2, although the HTLV-I provirus was already heavily methylated at the seroconversion. When DNA methylation of seroconverters was compared with that in carriers (Fig. 3A), provirus of carriers was more methylated in carriers than that of seroconverters ($p < 0.01$ by a Student's t-test) except for pol2 in seroconverter 2, and pX region. It suggests that DNA methylation of provirus accumulates during a latent period after seroconversion.

We established an HTLV-I-transformed cell line, ATL-21C, and cultured for over 9 years *in vitro*, and analyzed the DNA methylation of the HTLV-I provirus. Slight DNA methylation was detected in the *pol*, *env* and pX regions at 6 months after culture, however, it did not increase after 9 years. This indicates that the DNA methylation of HTLV-I provirus did not change after long-term *in vitro* culture (Fig. 4B). On the other hand, the *p16* gene in this cell line was not methylated at 6 months after culture, but heavily methylated after 9 years (data not shown). A comparison with the data from the seroconverters suggests that DNA methylation of the HTLV-I provirus tends to accumulate *in vivo*.

Association with DNA methylation in the neighboring host genome

It is possible that the HTLV-I provirus integrated into the heterochromatin or hypermethylated regions tends to be silenced [18], and that such HTLV-I-infected cells are selected in vivo. Therefore, we analyzed the DNA methylation of the host genome around the integration sites of the HTLV-I provirus. We first determined the integration sites of the HTLV-I provirus in ATL cells, and then analyzed the DNA methylation of genomic DNAs around the integration sites in both ATL cells and normal PBMCs from a non-carrier donor. When genomic DNAs neighboring integration sites were heavily methylated (Fig. 5), 5'-LTR was not methylated in three cases (acute ATL 1, 2 and 21) while they were methylated in two cases (acute ATL 3 and chronic ATL 1). In acute ATL 22, both genomic DNA and 5'-LTR were not so methylated. Thus, DNA methylation in the neighboring genomic regions was not correlated with the methylation status of the provirus among these cases.

Histone modification of the HTLV-I provirus

It has been demonstrated that DNA methylation of 5'-LTR is associated with histone deacetylation and silencing of viral gene transcription in cell lines [13]. When ATL-43T, in which tax gene transcription was silenced by hypermethylation of 5'-LTR, was compared with a tax gene-

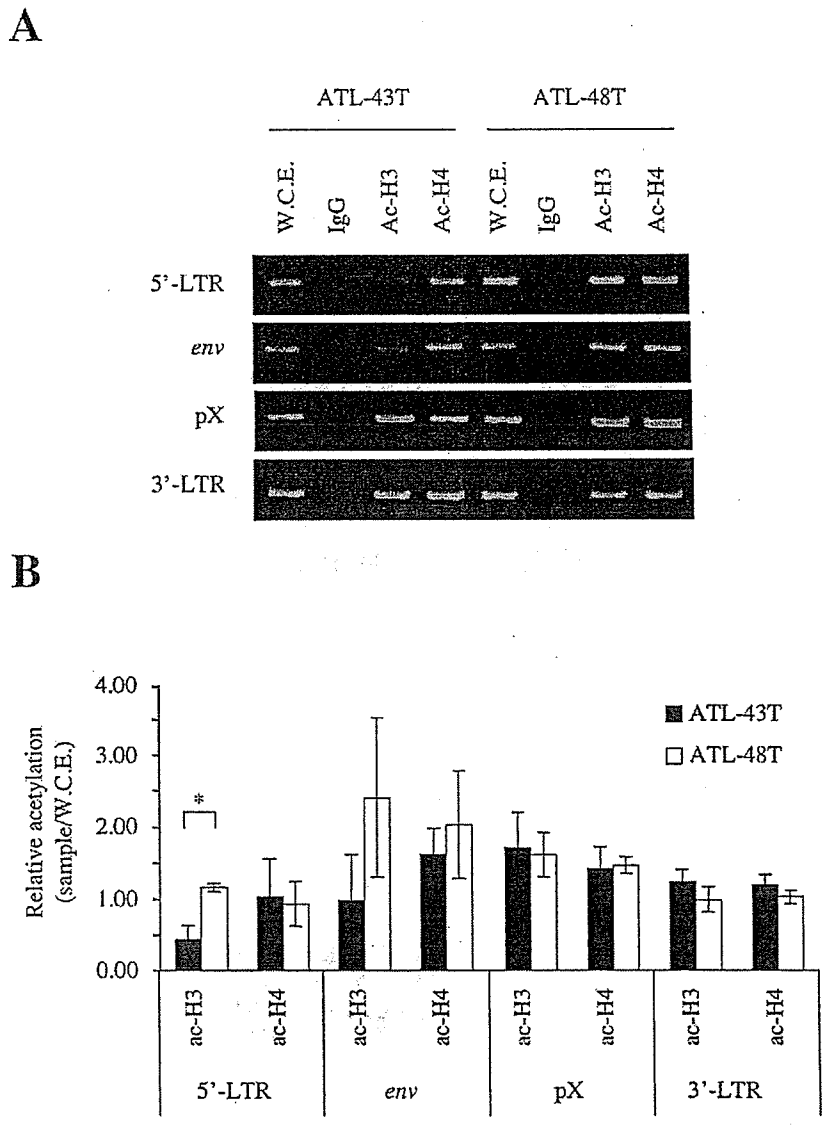

Figure 6
Histone modifications in ATL cell lines. Acetylation of histone was analyzed in *tax* gene-expressing (ATL-48T) and non-expressing (ATL-43T) cell lines by ChIP assays with anti-acetyl-Histone H3 or H4 (A and B) at four different regions (for 5'-LTR, *env*, pX and 3'-LTR) of the provirus. Representative data has been shown in A. W.C.E.: whole cell extract. ChIP assay was performed three times and quantified as described in Methods. Values are means ± SD(B). *:$p < 0.002$.